

# Multiply Charged Redox-Active Oligomers in the Gas Phase: Electrolytic Electrospray Ionization Mass Spectrometry of Metallocenes

Tracy Donovan McCarley,<sup>†</sup> Michael W. Lufaso,<sup>‡</sup> Larry S. Curtin,<sup>‡</sup> and Robin L. McCarley<sup>\*,†</sup>

*Choppin Laboratories of Chemistry, Louisiana State University, Baton Rouge, Louisiana 70803-1804, and Department of Chemistry, Youngstown State University, Youngstown, Ohio 44555-3663*

*Received: September 21, 1998*

The inherent constant-current electrolytic (CCE) nature of electrospray ionization mass spectrometry (ESI-MS) is used to study a variety of neutral metallocenes, including oligomeric metallocenes. ESI mass spectra that display the doubly charged ion of certain biferrrocenes ( $M^{2+}$ ) can be readily obtained by careful manipulation of solution conditions and structure of the biferrrocene. The intensity ratio of  $M^{2+}$  to the singly charged ( $M^+$ ) biferrrocene,  $I_{M^{2+}}/I_{M^+}$ , is strongly affected by the formal potentials of the two ferrocene sites ( $E^0_1$  and  $E^0_2$ ), the distance between the two redox centers, the analyte infusion (flow) rate, and concentration of the neutral metallocene. For a biferrrocene whose redox centers are well separated and  $E^0_1 \gg E^0_2$ , lower analyte concentrations and flow rates yield a higher  $I_{M^{2+}}/I_{M^+}$ , but the maximum achievable value is only 0.04. However, if the redox centers are physically well separated and  $E^0_1 \cong E^0_2$ , values of up to 0.3 for  $I_{M^{2+}}/I_{M^+}$  are attainable; through use of probability theory and  $I_{M^{2+}}/I_{M^+}$ , the electrochemical potential at the electrospray needle can be calculated. Multiply charged ions for several oligo(ferrocenyldimethylsilanes) are observed when electrolyte-containing solutions of the oligo(ferrocenyldimethylsilanes) are directly infused into the ESI source—in the case of the octa(ferrocenyldimethylsilane), the  $M^{4+}$  species is observed. To our knowledge, this is the first demonstration of ions with greater than two charges formed by electrolytic ESI-MS.

## Introduction

The analysis of polymers using mass spectrometry has been an active area of research for many years<sup>1</sup> but has recently experienced an explosive growth due to the advent of electrospray ionization mass spectrometry (ESI-MS)<sup>2</sup> and matrix-assisted laser desorption/ionization mass spectrometry (MALDI-MS).<sup>3</sup> Polar and nonpolar polymers have been investigated using ESI-MS and MALDI-MS, with the majority of the work focusing on sample preparation methods that lead to successful ionization and detection of protonated molecules or adduct ions without mass discrimination. Although many polar polymers have been studied with ESI-MS, there have been fewer ESI-MS investigations of nonpolar polymeric materials. Polymers and oligomers investigated to date include, for example, those derived from ethylene and propylene oxide, styrene, and methyl methacrylate.<sup>1</sup>

Recent work by Van Berkel<sup>4</sup> and Cole,<sup>5</sup> which was originally suggested by Kebarle,<sup>6</sup> indicates that materials that do not exist as preformed ions in solution can be ionized with an ESI source and observed in the gas phase if the materials can undergo electron-transfer reactions to yield stable product ions. Van Berkel has shown that ESI sources can be considered to be constant-current electrolytic (CCE) devices<sup>7,8</sup> that produce the ions necessary to provide charge compensation for the ESI process.<sup>4c-f</sup> This electrolytic process in ESI-MS is found to always operate, even when the analyte cannot undergo redox reactions. In such scenarios the electrolysis products ( $H^+$  from solvent electrolysis,  $Fe^{3+}$  from corrosion of the stainless steel

electrospray needle) often go undetected due to the fact that their presence does not greatly affect the mass spectrum of the analyte of interest. Studies by Cole and Van Berkel have shown that the addition of volatile electrolytes to redox analyte/solvent solutions can result in substantial increases in the observed ion abundance of the redox analyte of interest.<sup>4,5</sup> These pioneering studies have led to a number of fundamental electrolytic ESI-MS investigations of redox analytes such as metallocenes, porphyrins, carotenes, polycyclic aromatic hydrocarbons, fullerenes, heterocyclic and substituted aromatics, and quinones.<sup>4,5,9</sup> In addition, Van Berkel has gone on to show that doubly charged ions of metalloporphyrins may be observed if the analyte concentration and solution infusion rate are sufficiently low and the standard reduction potentials of the electron-transfer events are lower than the potential for oxidation of the electrospray needle.<sup>4e</sup>

An unexplored avenue of research that is certain to be developed is the use of the inherent constant-current electrolytic nature of ESI-MS in the characterization of conducting polymers.<sup>10-13</sup> Whether the conducting polymer is considered to be of the redox-hopping<sup>11</sup> or delocalized type,<sup>12</sup> ESI-MS should be very useful in gaining structural information about this very important class of polymeric materials. Applications for conducting polymers range from electrochromic display devices to chemical sensors.<sup>10,11,13</sup> Important to all of these applications and the fundamental studies associated with their development is an understanding of the structure and properties of the polymer at hand. Many of the conducting polymers initially investigated were prepared by methods that resulted in their formation and deposition (due to insolubility) onto the substrate that was used to initiate the polymerization reaction. Due to the intractable nature of these polymers, traditional methods for their characterization could not be applied. Thus,

\* To whom correspondence should be addressed. Phone (225) 388-3239; facsimile (225) 388-3458; e-mail tunnel@unix1.sncc.lsu.edu.

<sup>†</sup> Louisiana State University.

<sup>‡</sup> Youngstown State University.

establishing structure–property relationships was often trivial, and manipulation of a given polymer's structure in order to obtain a given physical characteristic was found to be a difficult, and sometimes impossible, undertaking. In an effort to more easily produce materials with desired properties, soluble conducting polymers with well-defined structures (known molecular weight distribution, geometry of monomer coupling) have been investigated.<sup>14</sup> Although methods such as gel-permeation chromatography and light scattering have been employed to obtain information regarding molecular weight and molecular weight distributions of soluble conducting polymers, these techniques do not offer a determination of absolute molecular weight.<sup>14k,l</sup> ESI-MS should be able to provide information on molecular weight and polydispersity of a variety of conducting polymers, as long as the ionized form of the polymer is easily achievable, stable, and soluble in the electrolyte medium.

We describe here initial ESI-MS investigations of dimeric metallocenes<sup>15</sup> and oligomeric<sup>16a</sup> metallocenes. A variety of polymeric metallocenes<sup>16b,17a</sup> have been investigated in solution and solid-state studies in order to gain knowledge concerning mass and charge transport mechanisms. For example, previous solution electrochemistry measurements in solvents such as tetrahydrofuran indicate that small molecular weight poly(vinylferrocenes),  $M_n < 5K$ , can have all the ferrocene sites oxidized without any noticeable precipitation of the multiply charged poly(vinylferrocenium) species. Higher molecular weight materials,  $M_n > 15K$ , exhibited voltammetry indicative of precipitation, even in solvents such as dimethylformamide which were expected to allow for adequate solubility of both the neutral and oxidized versions of the polymer. However, Manners has shown that poly(ferrocenylsilanes) do not form insoluble species upon electrochemical oxidation.<sup>16b</sup> Questions regarding the successful ionization and introduction of various poly(metallocenes) into the gas phase without precipitation or decrease in charge state caused us to first investigate ESI-MS of model dimeric and oligomeric metallocenes. Results from initial experiments with monomeric ferrocenes of varying formal potentials carried out with an electrospray ionization source of the Whitehouse design<sup>18</sup> demonstrate that this electrospray source design appears to operate in a controlled-current electrolytic mode—an observation consistent with that of Van Berkel and co-workers using a home-built electrospray ionization source with a different geometry than the source used in the investigations presented here. Studies with diferrocenylethane and biferrocenes with ferrocene groups bridged by alkane chains indicate that the analyte concentration and infusion rate, the distance between the charged ferrocene sites, and the formal potential,  $E^\circ$ , of the ferrocenes dictate the magnitude of the  $M^{2+}$  to  $M^+$  intensity ratio found in the ESI mass spectra. Multiply charged ions, up to  $M^{4+}$ , are observed for a series of oligo(ferrocenyldimethylsilanes). These results bode well for the analysis of conducting polymers that can be made to have multiple charges in solution, such as poly(metallocenes) and poly(heteroaromatics).

## Experimental Section

**Reagents.** Lithium trifluoromethanesulfonate (lithium triflate), ferrocenecarboxylic acid, ferrocene, bis(pentamethylcyclopentadienyl)iron, 1,2-diferrocenylethane, 7,7,8,8-tetracyanoquinodimethane, 2,3-dichloro-5,6-dicyano-1,4-benzoquinone, 2,3-benzanthracene, and nitrosonium tetrafluoroborate ( $\text{NOBF}_4$ ) were used as received from Aldrich. Gramicidin S was purchased from Sigma. Dichloromethane (Mallinckrodt) and acetonitrile (Burdick and Jackson) were nanograde and

spectrophotometric grades, respectively. Both 1,12-diferrocenyldodecane and 1,12-diferrocenyldodecan-1-one were made using slightly modified literature procedures.<sup>15a,19</sup> The oligo(ferrocenyldimethylsilanes) were provided by Professor Ian Manners at the University of Toronto.<sup>16a</sup>

**Procedure.** Stock solutions of electroactive analytes were prepared at 100  $\mu\text{M}$  in dichloromethane, and lithium triflate was prepared at 2.5 mM in acetonitrile. These solutions were combined and diluted with dichloromethane so that the final solutions for electrospray studies consisted of 10  $\mu\text{M}$  analyte and 0.25 mM lithium triflate in a solvent system of 9:1 (v:v) dichloromethane:acetonitrile (DCM:MeCN).

**Apparatus.** All electrospray mass spectra were obtained using a Finnigan MAT-900 double-focusing E–B arrangement mass spectrometer with an Analytica of Branford ESI source (early generation, 101-491-1) operated with nitrogen (Pre-Purified, BOC Gases,  $\text{H}_2\text{O}$  content  $\leq 3$  ppm) as the drying gas at a temperature of 130 °C. The standard stainless steel electrospray needle supplied by Analytica was used in all measurements; it has a length of 21.9 cm and an i.d. of  $1.02 \times 10^{-2}$  cm. Ions were detected using a PATRIC array detector during collection of all spectra. Analytes were introduced into the ESI source at flow rates of 0.8–3.0  $\mu\text{L min}^{-1}$  using a Harvard Apparatus syringe pump and a Gas-Tight Hamilton syringe. The mass spectrometer was calibrated using methanolic solutions of gramicidin S and/or diferrocenylethane dissolved in 0.25 mM lithium triflate in 9:1 dichloromethane:acetonitrile (DCM:MeCN). Spectra shown here typically consist of 10 co-added scans (time per scan is  $\sim 5$  s).

## Results and Discussion

**Establishing That the Analytica ESI Source Operates as a CCE Device.** The electrospray source of our mass spectrometer has the same design as the one developed by Whitehouse et al.<sup>18</sup> It has a stainless steel electrospray needle at atmospheric pressure that is grounded, and a heated glass desolvating capillary that has Au-coated ends. The end of the capillary that is closest to the needle is at atmospheric pressure and is held at  $-2000$  to  $-3000$  V in positive mode, while the other end of the capillary is contained within the vacuum system of the mass spectrometer leading to skimmers, focusing elements, and the mass analyzer. The electrical circuit of our source is different from those previously used to observe electrochemical reactions that result from the electrospray process.<sup>4,5</sup> In the particular sources used in those studies, the needle is held at  $+3000$  to  $+5000$  V in positive mode, and a stainless steel aperture plate of the mass spectrometer is held at ground. To ascertain whether the ESI source used here does indeed operate in an electrolytic mode, several electrochemically active metallocenes and quinones were analyzed by infusing submillimolar concentration solutions of the redox-active compound with added lithium triflate electrolyte. With the instrument operating in positive-ion mode (needle grounded and heated glass capillary held at  $-2000$  to  $-3000$  V), we were able to obtain mass spectra of various metallocenes (ranging from bis(pentamethylcyclopentadienyl)iron to 2,3-benzanthracene;  $-0.1 \text{ V} \leq E^0 \leq +0.98 \text{ V}$  vs SCE) that exhibited the molecular cation ( $M^+$ ). In addition, both 2,3-dichloro-5,6-dicyano-1,4-benzoquinone and 7,7,8,8-tetracyanoquinodimethane ( $E^0$  values of  $+0.62$  and  $+0.15 \text{ V}$  vs SCE, respectively) gave rise to spectra that displayed the molecular anion ( $M^-$ ) when the instrument was operated in negative-ion mode (needle grounded and capillary held at  $+2000$  to  $+3000$  V). Much lower intensity  $M^+$  and  $M^-$  signals or no signals whatsoever

were obtained for all of the analytes investigated when no lithium triflate was added to the infusion medium. In addition, large increases in the infusion rate resulted in the observation of lower absolute ion intensities. The time that the analyte resides in the needle,  $t_E$ , can be computed using eq 1

$$t_E = \pi r_n^2 L / \nu \quad (1)$$

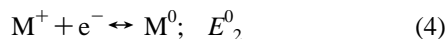
where  $r_n$  is the inside radius of the needle,  $L$  is the length of the needle, and  $\nu$  is the volumetric flow rate.<sup>4,7</sup> One can also calculate the time needed for the analyte to diffuse from the center of the needle to the needle wall using the Einstein equation

$$t_D = r_n^2 / 2D_k \quad (2)$$

where  $D_k$  is the solution diffusivity of the particular analyte.<sup>4,7</sup> As long as the applied current is sufficient and  $t_E$  is larger than  $t_D$ , there will be adequate time for all of the analyte to diffuse to the wall of the electrospray needle and undergo electron-transfer reactions before it exits the needle. However, large increases in the flow rate should result in decreased electrolysis of the analyte ( $t_E < t_D$ ), leading to lower absolute ion intensities. Taken collectively, the Analytica ESI source appears to operate as a constant-current electrolytic device. This is further substantiated in the discussion below concerning biferrocenes.

**ESI-MS of Biferrocenes and the Quest for  $M^{2+}$ :** **Biferrocenes Containing Inequivalent Redox Sites.** One of the major concerns in the application of ESI-MS to the routine analysis of high molecular weight redox-conducting polymers is whether multiply charged polymer ions can be observed in the gas phase with an unmodified (stainless steel needle is standard), commercial ESI source. Some of these polymers will contain electroactive sites with fairly high standard redox potentials ( $E^0$ ) and different standard potentials. Other concerns regarding the successful observation of multiply charged poly-(redox site) ions in the gas phase include reduced solubility of the highly charged polymeric material in the infusion medium and gas-phase reactions that could possibly reduce the charge state of the polymeric species.

To gain a better understanding of some of the possible limitations that one may encounter during the analysis of metallocene polymers, we first investigate and discuss the properties of a series of biferrocenes. We consider here, for the discussion at hand, a molecule  $M$  with two redox centers (two different molecular orbitals) which can form a dication  $M^{2+}$  and whose formal potentials for the two individual one-electron-transfer events ( $E_1^0$  and  $E_2^0$ )



are such that comproportionation reactions between  $M^{2+}$  and  $M^0$  are highly favorable ( $M^{2+} + M^0 \rightarrow 2M^+$ ;  $E_1^0 > E_2^0$ ). This is the classical  $E_rE_r$  reaction.<sup>7</sup> Under these limitations there are several ways in which to ensure the production of multiply charged ions when carrying out ESI-MS on redox-active species. Low analyte concentrations, reasonable supporting electrolyte concentrations, and low analyte infusion rates have been shown to be conducive to the formation of doubly charged ions ( $M^{2+}$ ), such as those observed for metalloporphyrins.<sup>4c</sup> The rationale for use of these parameters is straightforward if one considers the ESI source to be a CCE flow cell with a working electrode of fixed surface area.<sup>7</sup> Assuming that the concentration of

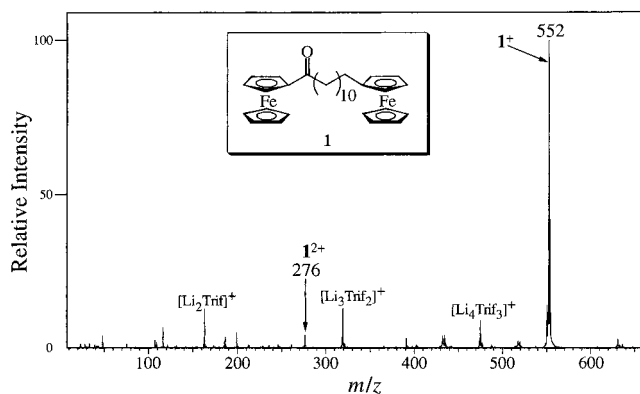
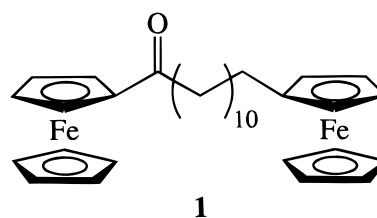


**Figure 1.** ESI mass spectrum of  $10 \mu\text{M}$  **1** with  $0.25 \text{ mM}$  lithium triflate (LiTrif) in  $9:1$  dichloromethane:acetonitrile (DCM:MeCN) at an infusion rate of  $0.8 \mu\text{L min}^{-1}$ . ESI voltage =  $-2627 \text{ V}$  and current =  $60 \text{ nA}$ .

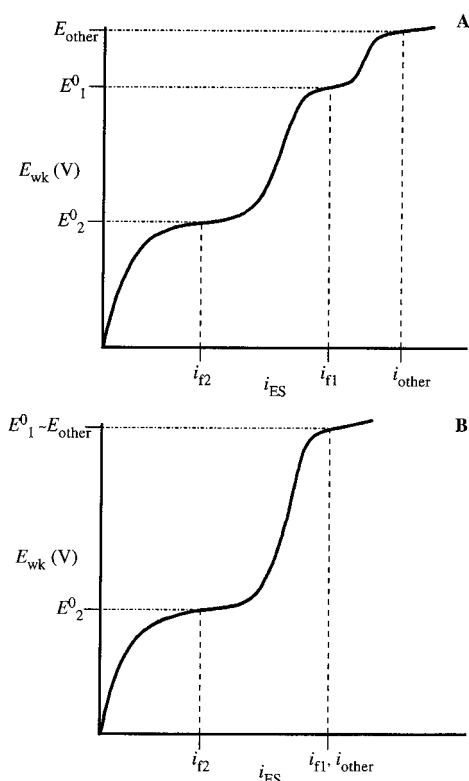
electrolyte is sufficient to sustain a fixed faradaic current,  $i_f$ , and the  $M^{2+}$  form of the analyte is chemically stable in solution (no follow-up reactions or precipitation),  $M^{2+}$  should be produced if the amount of time the analyte remains in the electrolysis cell,  $t_E$ , is  $\sim 2$  times greater than the diffusion time necessary for the analyte to move from the center of the flow stream to the solution/electrode interface,  $t_D$ .<sup>20</sup> In such a scenario it makes complete thermodynamic sense that there will be no  $M^{2+}$  in the eluate from the flow cell until all of the neutral  $M^0$  is consumed within the flow cell, even if the potential of the electrode (in our case the electrospray needle) could be made large enough to produce  $M^{2+}$  at the electrode/solution interface. The aforementioned points have been well demonstrated by Van Berkel and co-workers during their experiments that employed both stainless steel and platinum ESI needles and analytes whose formal potentials differed by several tenths of a volt ( $\Delta E^0 = E_2^0 - E_1^0 \cong -0.5 \text{ V}$ ).<sup>4e</sup>

To assess the effects of redox center inequivalence on the ability to observe the doubly charged species of a biferrocene, ESI-MS studies of **1** were undertaken. The two ferrocene groups in **1** undergo electron transfer at quite different standard



potentials ( $E_1^0 = +0.54 \text{ V}$  and  $E_2^0 = +0.24 \text{ V}$  vs SCE). A representative positive-ion electrospray mass spectrum of  $10 \mu\text{M}$  **1** with  $0.25 \text{ mM}$  lithium triflate (LiTrif) in  $9:1$  dichloromethane:acetonitrile (DCM:MeCN) at an infusion rate of  $0.8 \mu\text{L min}^{-1}$  is shown in Figure 1. Although ions for  $[\text{Li}_y(\text{Trif})_{y-1}]^+$  clusters are apparent, the major ion present is the molecular ion,  $M^+$ , of **1** at  $m/z$  552. Also apparent is an ion at  $m/z$  276. Careful inspection of the region near  $m/z$  276 revealed A and A + 1 peaks with  $0.5 \text{ amu}$  spacing indicative of  $1^{2+}$ . Increases in flow rate led to decreases in the intensity of  $1^{2+}$  relative to that of  $1^+$ . At the flow rate used in Figure 1, an electrolysis time  $t_E$  of  $133 \text{ s}$  is calculated, while  $t_D$  is found to be  $2.6 \text{ s}$  when using a conservative  $D_k$  value of  $5 \times 10^{-6} \text{ cm}^2 \text{ s}^{-1}$ . Although the electrolysis time exceeded the diffusion time by more than 50-fold in this experiment, the ratio of  $1^{2+}$  to  $1^+$  is a mere  $0.04$ .

## SCHEME 1



A possible explanation for the small amount of  $\mathbf{1}^{2+}$  observed at flow rates that should allow for its abundant production is preferential oxidation (corrosion) of the stainless steel electro-spray needle in comparison to oxidation of  $\mathbf{1}$  to  $\mathbf{1}^{2+}$ . This proposal is supported upon comparison of the amount of faradaic current needed to convert all of  $\mathbf{1}$  to  $\mathbf{1}^{2+}$ ,  $i_f$ , to the measured electro-spray current,  $i_{ES}$ , and voltammetry at a stainless steel wire electrode in the dichloromethane:acetonitrile solvent used here. The faradaic current needed for complete conversion of a redox species  $k$  to a given charge state involving  $n$  electrons in a flow cell with analyte volumetric flow rate  $\nu$  is given by

$$i_f = \sum_k n_k C_k^b F \nu \quad (5)$$

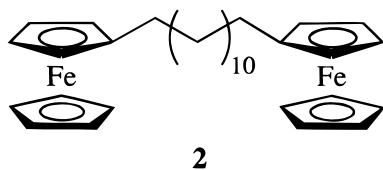
where  $C_k^b$  is the concentration of the redox species to be oxidized and  $F$  is the Faraday constant.<sup>4c</sup> Such a calculation under the conditions in Figure 1 yields a value of 26 nA for the complete conversion of  $\mathbf{1}$  to  $\mathbf{1}^{2+}$ . The measured  $i_{ES}$  was 60 nA, a value far in excess of the faradaic current needed for complete conversion of  $\mathbf{1}$  to  $\mathbf{1}^{2+}$  when  $t_E > t_D$ . Due to the fact that  $i_{ES}$  must equal  $i_f$  for the constant-current electrolysis cell,<sup>4c,6</sup> there must be other reactions that satisfy  $i_f$  besides those associated with the oxidation of  $\mathbf{1}$ . This scenario is depicted in Scheme 1. It can be seen that the potential of the electro-spray needle (working electrode)  $E_{wk}$  will adopt an average value that will cause redox reactions to occur at a rate so as to satisfy  $i_{ES}$ . If the current supplied by oxidation of  $\mathbf{1}$  to  $\mathbf{1}^{2+}$  is not sufficient to satisfy  $i_{ES}$ , the potential will rise to the potential  $E_{other}$  such that another component in the system will be oxidized so as to satisfy  $i_{ES}$ . This change in  $E_{wk}$  to  $E_{other}$  can only occur if *all* of  $\mathbf{1}$  is converted to  $\mathbf{1}^{2+}$  (Scheme 1A), *unless*  $E_{other}$  is very close to  $E^0_1$ . Under conditions in which  $E_{other}$  is very close to  $E^0_1$  (Scheme 1B), the other reactions at  $E_{other}$  may occur in preference to the oxidation of  $\mathbf{1}$  to  $\mathbf{1}^{2+}$  if the concentration of the other species is large. Such a scenario would lead to lower

conversion of  $\mathbf{1}^+$  to  $\mathbf{1}^{2+}$ , even when  $t_E \gg t_D$ . Van Berkel has shown that oxidation of the stainless steel electro-spray flow cell (the other reaction) occurs instead of the oxidation of a solution-phase metalloporphyrin, due to the fact that the potential for oxidation of the metalloporphyrin ( $E^0 = +0.76$  V vs SCE) is very near that of the onset of oxidation of stainless steel in dichloromethane electrolyte ( $\sim +0.8$  V vs SCE).<sup>4e</sup> Experiments in our laboratory at a 306 stainless steel wire indicate that the potential at which the stainless steel begins to oxidize ( $E_{SS}$ ) in 9:1 dichloromethane:acetonitrile is near +0.5 V vs SCE, which is 0.04 V negative of  $E^0_1$  for  $\mathbf{1}$ . Thus, with such a small difference in the values for  $E^0_1$  and  $E_{SS}$ , one would expect that the oxidation of the stainless steel electro-spray needle *would* occur in preference to the oxidation of  $\mathbf{1}^+$  to  $\mathbf{1}^{2+}$ , leading to a situation similar to that of Scheme 1B. Such a situation would lead to poor analyte conversion efficiency and an inability to completely electrolyze  $\mathbf{1}^+$  to  $\mathbf{1}^{2+}$ , even when  $t_E \gg t_D$ . The conversion efficiency may also be possibly hindered further by nonuniform current densities along the length of the electro-spray needle, which would result in a decreased electrolysis volume and thus a lower amount of  $\mathbf{1}^+$  converted to  $\mathbf{1}^{2+}$ . Van Berkel has noted that stainless steel electro-spray flow cells exhibit corrosion pits near the outlet of the flow cell after use<sup>21</sup> and, similar to our observations, has found that incomplete redox conversion occurs in an electro-spray flow cell when (1) the measured  $i_{ES}$  is greater than the faradaic current needed for the conversion of analyte and (2) the calculated  $t_E$  is greater than  $t_D$ .<sup>4e</sup> At this point in time we can only speculate about the nonuniform current density along the length of the electro-spray needle. We conclude that the small amount of  $\mathbf{1}^{2+}$  observed at flow rates that should allow for its abundant production is due to preferential oxidation of the stainless steel electro-spray needle. Thus, it is necessary for  $\mathbf{1}$  to remain in the electro-spray source longer than the theoretical value of  $t_E$  in order to achieve production of  $\mathbf{1}^{2+}$ .

**Biferrocenes Containing Equivalent Redox Sites: Long Tether between Ferrocenes.** It is expected that molecules containing two identical, *noninteracting* redox sites should give rise to ESI mass spectra that exhibit the  $M^{2+}$  ion at  $t_E$  values much smaller than those needed for production of species such as  $\mathbf{1}^{2+}$ . This expectation comes from theoretical and experimental studies of multielectron-transfer reactions of dimers<sup>15b,17b</sup> and polymers<sup>16b,17a</sup> containing noninteracting “monomer” redox sites. Redox sites in molecules such as the aforementioned can undergo successive electron-transfer reactions, otherwise known as  $E_r E_r E_r \dots$  reactions. Each monomer site in these molecules has the same standard potential,  $E^0_m$ , and obeys the Nernst equation without regard for the redox state of the other sites. However, the potential for each electron transfer will not be  $E^0_m$  but rather the formal potential for the *successive* electron transfer,  $E^F_j$ , which is the result of entropic (statistical) effects. That is to say, the formal potential associated with a given electron-transfer reaction for a molecule with  $j$  reduced sites will depend on the total number of redox centers (sites),  $n$ , in the molecule. Bard and Anson have shown that the formal potential for each pair of the successive redox states can be calculated using eq 6.<sup>17a</sup>

$$E^F_j = E^0_m - \frac{RT}{F} \ln \left[ \frac{j}{n-j+1} \right] \quad (6)$$

For example, a molecule such as  $\mathbf{2}$  that has two redox centers with  $E^0_m = +0.242$  V vs SCE will have a formal potential for the 1+/0 couple,  $E^F_2$ , of +0.224 V and  $E^F_1 = +0.260$  V for the 2+/1+ couple at 298 K. The difference in formal potentials



between the first and last redox states can be calculated from<sup>17a</sup>

$$\Delta E^F = E_n^F - E_1^F = -\left[\frac{2RT}{F}\right] \ln n \quad (7)$$

with all terms having the same meaning as in eq 6. For a molecule containing two noninteracting redox centers, the difference in formal potentials for the 1+/0 and 2+/1+ couples is calculated to be  $-36$  mV at 298 K. In addition, the difference in the successive formal potentials will become increasingly smaller as the number of redox centers becomes greater in a molecule. Thus, small changes in the potential of the working electrode  $E_{wk}$  will dramatically affect the population of the various charge states. The population of a given charge state (with  $j$  reduced centers),  $f_j$ , as a function of  $E_{wk}$  for a molecule containing multiple redox sites can be calculated using<sup>17a</sup>

$$f_j = \binom{n}{j} \left[ \frac{\theta}{1+\theta} \right]^{n-j} \left[ \frac{1}{1+\theta} \right]^j \quad (8)$$

$$\theta = \exp\left[\frac{F(E - E_m^0)}{RT}\right] \quad (9)$$

where  $\binom{n}{j}$  is defined as  $n!/j!(n-j)!$ . The high sensitivity of the charge state population to changes in  $E_{wk}$  for the case of a dimer containing noninteracting, equivalent redox centers is shown in Figure 2. Such subtle variations in  $E_{wk}$  in the electro spray working electrode (needle) will come about by small changes in the analyte infusion rate. From an examination of the theory for hydrodynamic voltammetry and constant-current potentiometry, the dependence of  $E_{wk}$  on  $\nu$  is predicted to be linear, with the potential becoming more negative with increasing flow rate.<sup>22</sup> Thus, it should be possible to observe multiply charged species without the use of exceedingly small flow rates, and the population of the charge states should be strongly affected by flow rate.

Shown in Figure 3A is the ESI mass spectrum of  $10 \mu\text{M}$  **2** with  $0.25 \text{ mM}$  LiTrif in 9:1 DCM:MeCN at an infusion rate of  $0.8 \mu\text{L min}^{-1}$ . The major ion in the spectrum is  $2^+$  at  $m/z$  538, but  $2^{2+}$  is readily apparent at  $m/z$  269. Calculations yield  $t_E = 133 \text{ s}$  and  $t_D = 2.6 \text{ s}$  ( $D_k = 5 \times 10^{-6} \text{ cm}^2 \text{ s}^{-1}$ ) for  $\nu = 0.8 \mu\text{L min}^{-1}$ . When comparing the ratio of the ion intensities,  $I_{M^{2+}}/I_{M^+}$ , for **1** and **2** at  $\nu = 0.8 \mu\text{L min}^{-1}$ , one finds values of 4% and 29%, respectively. This large difference in the relative abundance of the  $M^{2+}$  for **1** and **2** can be explained by considering, as discussed above, the fact that the two ferrocene centers in **2** are equivalent, noninteracting sites (voltammogram displays only one wave), while those in **1** are noninteracting but certainly have much different standard reduction potentials ( $\Delta E^0 = -300 \text{ mV}$ ). One can calculate the value of the comproportionation constant  $K_{\text{comp}}$  for the reaction of  $M^{n+} + M^{(n-2)+} \rightarrow 2M^{(n-1)+}$  ( $x$  being the valence) from eq 10

$$K_{\text{comp}} = \exp\left[\frac{-\Delta E^F}{RT}\right] \quad (10)$$

with  $\Delta E$  being either  $\Delta E^F$  or  $\Delta E^0$  and all other terms having the same meaning as in eq 6. The value of  $K_{\text{comp}}$  based on  $\Delta E^0 = -300 \text{ mV}$  is  $1.2 \times 10^5$  for **1**, while a similar calculation

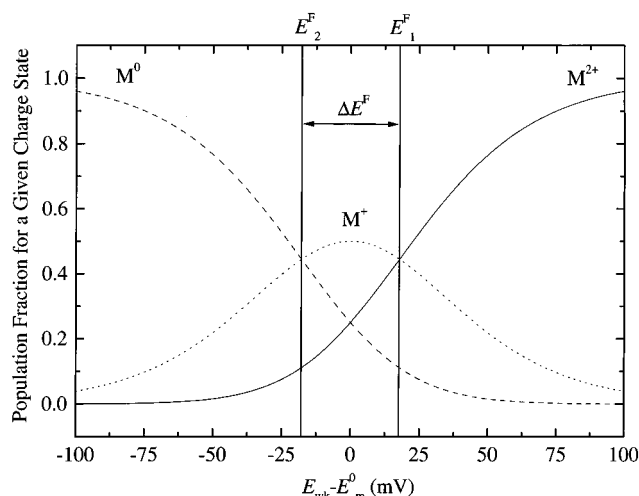


**Figure 2.** Calculated populations of the  $M^{2+}$ ,  $M^+$ , and  $M^0$  states of a dimer containing noninteracting, equivalent redox centers as a function of the working electrode potential. The calculations were obtained by use of eq 8.

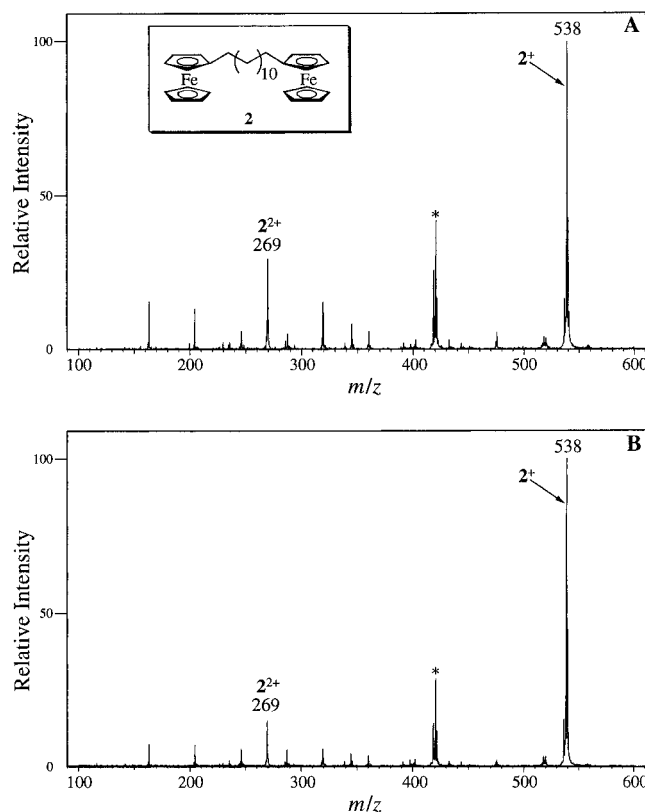


**Figure 3.** ESI mass spectra of  $10 \mu\text{M}$  **2** with  $0.25 \text{ mM}$  lithium triflate (LiTrif) in 9:1 dichloromethane:acetonitrile (DCM:MeCN) at an infusion rate of  $0.8 \mu\text{L min}^{-1}$  (A) and  $1.0 \mu\text{L min}^{-1}$  (B). ESI voltage =  $-2195 \text{ V}$  and current =  $75 \text{ nA}$  for both (A) and (B). The ions marked with an asterisk at 418 and 420 are two different ferrocene-containing impurities formed during the synthesis of **2**—these are indeed impurities and not fragments formed during the electro spray process, for the presence of these species in the stock solution has been confirmed using gas chromatography/mass spectrometry (electron impact).

yields a  $K_{\text{comp}}$  of only 4.1 for **2** ( $\Delta E^F$  assumed to be  $-36 \text{ mV}$ ). Even if the potential of the electro spray needle could be made so as to produce  $1^{2+}$  (no corrosion of the needle), as long as there is  $1^0$  remaining in the needle, comproportionation reactions would preclude its observation.

As proposed above, slight variations in analyte infusion rate should result in large changes in the solution concentration of

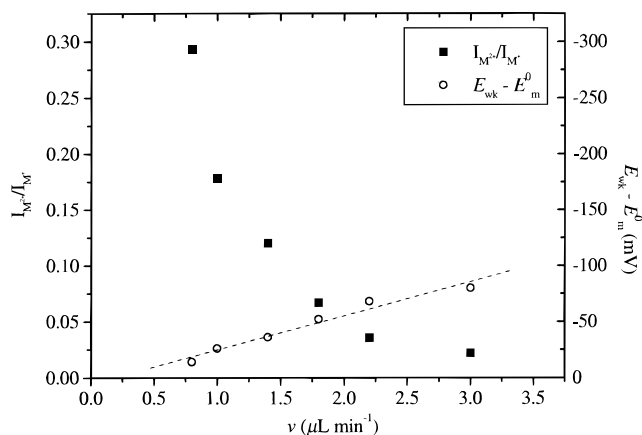
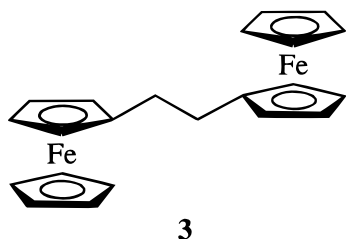


**Figure 4.** Plots of observed  $I_{2^+}/I_2^+$  (■) and calculated  $E_{wk}$  (○) as a function of analyte infusion rate. The dashed line represents the line obtained by linear regression analysis of the  $E_{wk}$  vs  $v$  plot; the correlation coefficient for the fit was found to be 0.983.

$2^0$ ,  $2^+$ , and  $2^{2+}$  and be reflected by changes in the ion intensities of the various charge states in the gas phase, assuming that no discrimination of ions of a given charge or charge reducing reactions occur as the ions enter the gas phase. As is evident from comparing parts A and B of Figure 3, the change in  $I_{2^+}/I_2^+$  upon increasing the flow rate from  $0.8 \mu\text{L min}^{-1}$  ( $t_E = 133$  s) to  $1.0 \mu\text{L min}^{-1}$  ( $t_E = 107$  s) is striking; a 40% decrease in  $I_{2^+}/I_2^+$  was obtained. The variation in  $I_{2^+}/I_2^+$  as a function of infusion rate is displayed in Figure 4 (■). Assuming that there are no charge-altering reactions or ion discrimination effects upon transfer of solution-phase ions to the gas phase,  $I_{1^+}/I_1^+$  can be used with eq 8 to obtain an estimate of  $E_{wk}$  at the different flow rates.<sup>23</sup> The results from such calculations are plotted as a function of flow rate in Figure 4 (○). As expected,  $E_{wk}$  becomes more negative as the flow rate is increased. Values of  $E_{wk}$  range from  $-14$  to  $-80$  mV for flow rates of  $0.8$ – $3.0 \mu\text{L min}^{-1}$ . Although previous ESI-MS investigations of a variety of redox-active analytes have presented strong support for the approximate value of  $E_{wk}$  during ESI-MS experiments,<sup>4–6,9</sup> the work described here is to our knowledge the first assessment of the approximate value of  $E_{wk}$  during the constant-current electrolysis of a redox compound in an ESI source.<sup>23</sup>

**Biferrocenes Containing Equivalent Redox Sites: Short Tether between Ferrocenes.** To explore the effects of redox center separation distance on the observed mass spectra of a bimetalloocene that displays solution voltammetry indicative of noninteracting redox centers, 1,2-diferrocenyloethane (**3**) was



examined under conditions identical to those used for analysis of compounds **1** and **2**. Compound **3** is known to give rise to solution-phase voltammograms consisting of an unresolved two-electron wave.<sup>15b</sup> Our choice of **3** is based on the fact that, unlike **1** and **2**, there exists a strong possibility that the proximity of the two charges on the  $M^{2+}$  species may result in decreased stability of the doubly charged ion and reactions that reduce the charge state upon transfer to the gas phase. The ESI mass

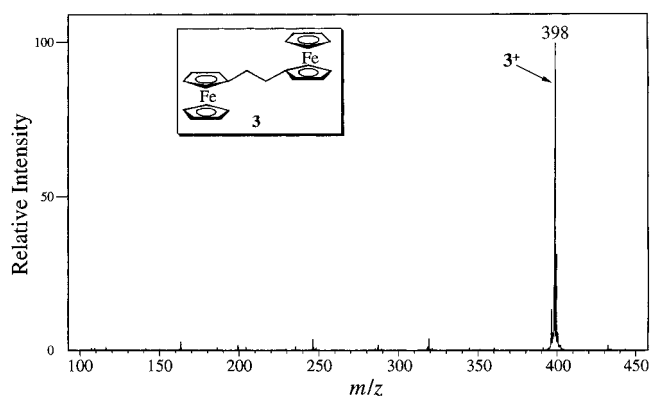


**Figure 5.** ESI mass spectrum of  $10 \mu\text{M}$  **3** with  $0.25 \text{ mM}$  lithium triflate (LiTrif) in  $9:1$  dichloromethane:acetonitrile (DCM:MeCN) at an infusion rate of  $0.8 \mu\text{L min}^{-1}$ . ESI voltage =  $-3076$  V and current =  $50$  nA.

spectrum of  $10 \mu\text{M}$  **3** with  $0.25 \text{ mM}$  LiTrif in  $9:1$  DCM:MeCN at an infusion rate of  $0.8 \mu\text{L min}^{-1}$  is shown in Figure 5. Besides the aforementioned background ions, a molecular ion,  $M^+$ , of **3** at  $m/z$  398 is observed. An ion at the same  $m/z$  as that expected for  $3^{2+}$  ( $m/z$  199) was observed, and its intensity could be altered by variations in the applied skimmer-cone voltage. Separation of the A and A + 1 peaks by 1 amu (rather than 0.5 amu) indicates that the ion at  $m/z$  199 formed under these conditions is not due to  $3^{2+}$  but rather a fragment ion, presumably  $\text{C}_5\text{H}_5\text{FeC}_5\text{H}_4\text{-CH}_2^+$ . Variations in analyte and electrolyte concentration, infusion rate, and electrospray voltage did not result in observation of  $3^{2+}$ . This result is surprising considering that the  $E^0$  of **3** is  $+0.26$  V vs SCE (virtually identical to **2**), and the  $M^{2+}$  of **2** was observed in the gas phase under almost identical conditions. We present four possible explanations for the inability to observe  $3^{2+}$  using the conditions described here: (1) Production of  $3^{2+}$  does not occur at the stainless steel electrode/solution interface. (2) The solubility of  $3^{2+}$  is extremely low. (3) The reactivity of  $3^{2+}$  in solution is such that it decomposes. (4) A decrease in charge state occurs for  $3^{2+}$  upon entering the gas phase. Possibility 3 can be ruled out immediately based on the well-established stability of the dication of **3** in organic electrolyte solutions.<sup>15b</sup> In addition, voltammetry of **3** in  $\text{Bu}_4\text{NBF}_4/\text{DCM}$  at a platinum electrode performed in our laboratories does not indicate any precipitation (possibility 2). Even though we have not attempted to carry out voltammetry of **3** at a stainless steel electrode, it would seem impossible that  $3^{2+}$  would not be formed at the stainless steel electrospray needle, particularly when molecules such as **2** are electrolyzed to form  $2^{2+}$  under identical conditions (possibility 1). This leaves the possibility that is concerned with a decrease in charge state for  $3^{2+}$  upon entering the gas phase—if any  $3^{2+}$  is produced in the electrospray needle, then charge altering reactions may prevent its appearance in the mass spectrum.<sup>24</sup>

To test the hypothesis that charge-reduction reactions result in a decrease in charge state for  $3^{2+}$  upon entering the gas phase, solutions of diferrocenyloethane with various amounts of added nitrosonium tetrafluoroborate were infused into the ESI source.  $\text{NO}^+$  is a well-known oxidant capable of oxidizing materials with formal potentials as high as  $\sim +0.7$  V vs SCE.<sup>25</sup> When  $\text{NO}^+$  was added to the diferrocenyloethane solutions, a blue color developed immediately, indicating the presence of ferrocenium species. Upon addition of  $\sim 1.1$  equiv of  $\text{NO}^+$  to a solution of **3**, the spectrum in Figure 6A was obtained. A small amount of  $3^{2+}$  at  $m/z$  199 was produced by use of the chemical oxidant, as noted by the separation of the A and A + 1 peaks by 0.5 amu. Additional amounts of added  $\text{NO}^+$  resulted in steady

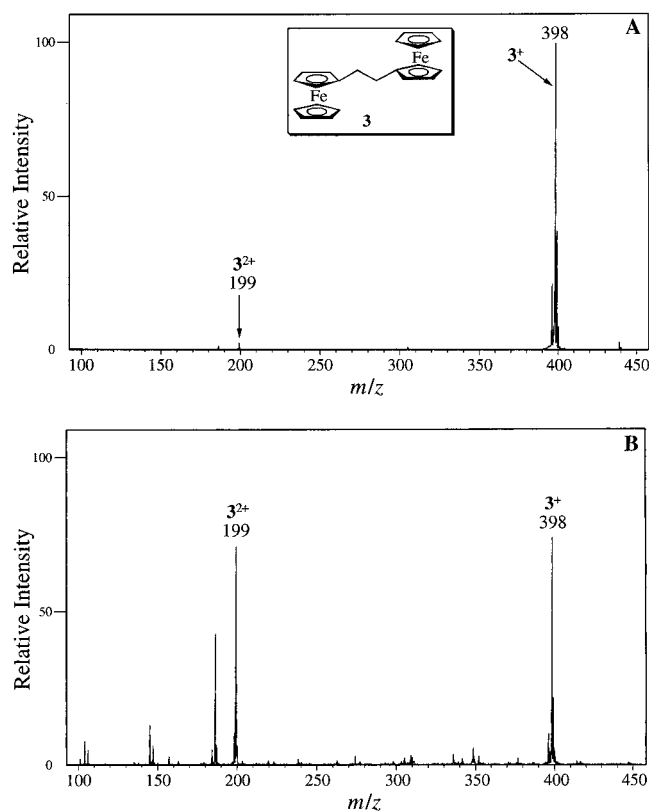


**Figure 6.** ESI mass spectra of  $900\ \mu\text{M}$  **3** with  $0.25\ \text{mM}$  lithium triflate (LiTrif) in 9:1 dichloromethane:acetonitrile (DCM:MeCN) at an infusion rate of  $1.7\ \mu\text{L}\ \text{min}^{-1}$ . The spectra were obtained with 1.1 (A) and 4 equiv (B) of added  $\text{NOBF}_4$ .

increases in the intensity ratio of  $3^{2+}$  to  $3^+$ . The spectrum obtained after the addition of 4 equiv of  $\text{NO}^+$  is shown in Figure 6B. With this much added oxidant (2 times that needed for complete conversion of **3** to  $3^{2+}$ ), one would expect that there would be no observable singly charged molecular ion,  $\text{M}^+$ , of diferrocenylolethane. However,  $\text{M}^+$  is observed, and in fact, the ratio of  $\text{M}^+$  to  $\text{M}^{2+}$  is very large (0.74). This result indicates that there must be a pathway for re-forming  $3^+$  from  $3^{2+}$ . At this time, the reactions that lead to the loss of  $3^{2+}$  upon transfer to the gas phase are not known. It is certainly possible that, as the doubly charged species enters the gas phase and loses solvent, increased electrostatic interactions between the closely spaced ferrocenium groups result in an increase in the effective oxidative capabilities of  $3^{2+}$ , leading to the formation of  $3^+$  through reactions of  $3^{2+}$  with the electrolyte/solvent. A similar electrostatic argument has been used to rationalize the apparent change in the  $\text{p}K_a$  and the corresponding change in charge state, upon introduction to the gas phase, for analytes formed by acid/base reactions in solution.<sup>24</sup> Whatever the reason, our data support the idea that a decrease in the distance between equivalent redox centers results in a decrease in the amount of observable  $\text{M}^{2+}$  in the gas phase. This is an important observation due to the fact that the maximum charge state achievable for a polymeric metallocene using ESI-MS may be limited, thus decreasing the applicability of ESI-MS to the analysis of high molecular weight polymers. In addition, we must state that it is possible that some charge-reducing reactions occur during analysis of **2**, causing our determinations of  $E_{\text{wk}}$  to be in error. This is discussed in further detail below.

**ESI-MS of Oligo(ferrocenyldimethylsilanes).** To investigate the maximum attainable charge state for a multicenter redox molecule in the gas phase using the commercial ESI source, a series of well-defined oligo(ferrocenyldimethylsilanes)<sup>16a</sup> were

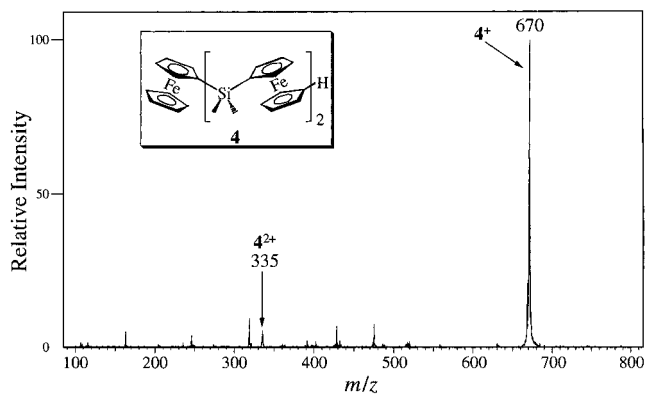
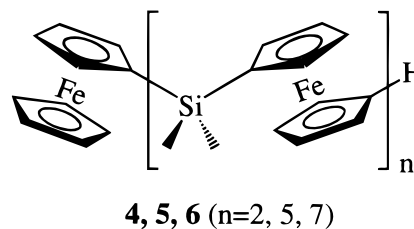


**Figure 7.** ESI mass spectrum of  $10\ \mu\text{M}$  **4** with  $0.25\ \text{mM}$  lithium triflate (LiTrif) in 9:1 dichloromethane:acetonitrile (DCM:MeCN) at an infusion rate of  $0.8\ \mu\text{L}\ \text{min}^{-1}$ . ESI voltage =  $-2452\ \text{V}$  and current =  $55\ \text{nA}$ .

investigated. It has been shown in solution voltammetry studies that the  $n = 2$  ferrocenyldimethylsilane oligomer **4** undergoes



two voltammetrically indistinguishable ( $\sim 60\ \text{mV}$  separation) one-electron transfers with  $E_{1/2} = +0.30\ \text{V}$  vs SCE, followed by a well-separated one-electron process with  $E_{1/2} = +0.53\ \text{V}$  vs SCE. The overall process can be envisioned as every other ferrocene site (the “end” ferrocenes) being oxidized first, followed by oxidation of the “sandwiched” or central ferrocene. The  $E_{1/2}$  value of the central ferrocene is much greater than that of the end ferrocenes due to the effects associated with being sandwiched between two cations. Based on the difference in  $E_{1/2}$  values for production of  $4^{2+}$  and  $4^{3+}$  ( $0.23\ \text{V}$ ), the results observed for compounds **1** and **2**, and the nature of the CCE process at the electrospray needle, one would expect that the ESI mass spectra would display only the  $\text{M}^{2+}$  and  $\text{M}^+$  states. In other words, all of  $4^+$  and  $4^0$  would have to be completely consumed in the electrolysis volume of the needle in order to observe  $4^{3+}$ . Such a large amount of electrolysis would not seem possible at the stainless steel needle used here, as noted by the results obtained for **2** (lack of complete conversion of  $2^+$  to  $2^{2+}$  at similar flow rates), unless flow rates lower than that needed to sustain a stable spray could be used. In fact, only  $4^+$  and  $4^{2+}$  were observed, as evidenced by the spectrum in Figure 7 and others obtained when a variety of experimental parameters were changed. Whether or not  $4^{3+}$  can be observed using a platinum needle is yet to be seen, but its observation may not be possible due to the results noted above for **1** and **3**. As was found for **2**, the ratio of the ion intensities of the doubly charged to singly charged species of **4** was strongly dependent on infusion rate, demonstrating the previously discussed effect of flow rate on  $E_{\text{wk}}$ .

We turn our discussion to the ESI-MS of **5** and **6**, the  $n = 5$  and  $n = 7$  ferrocenyldimethylsilane oligomers. Voltammetry of these two compounds has demonstrated that the hexamer **5** ( $n = 5$ ) exhibits an unresolved three-electron wave and the octamer **6** ( $n = 7$ ) an unresolved four-electron wave at  $E_{1/2} \sim +0.30\ \text{V}$  vs SCE. A subsequent one-electron wave at  $E_{1/2} \sim$

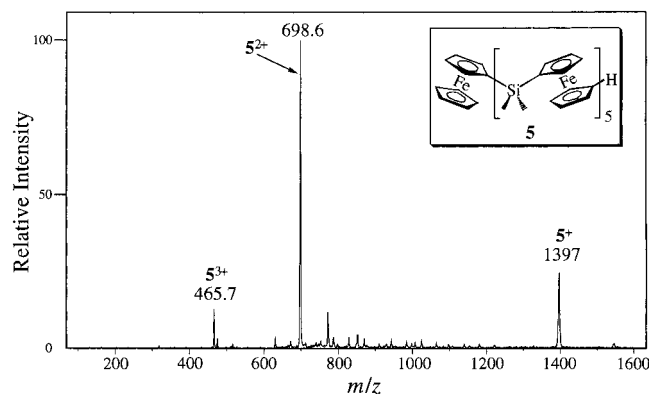


**Figure 8.** ESI mass spectrum of 5  $\mu\text{M}$  **5** with 0.25 mM lithium triflate (LiTrif) in 9:1 dichloromethane:acetonitrile (DCM:MeCN) at an infusion rate of 1.0  $\mu\text{L min}^{-1}$ . ESI voltage =  $-2314$  V and current = 60 nA.

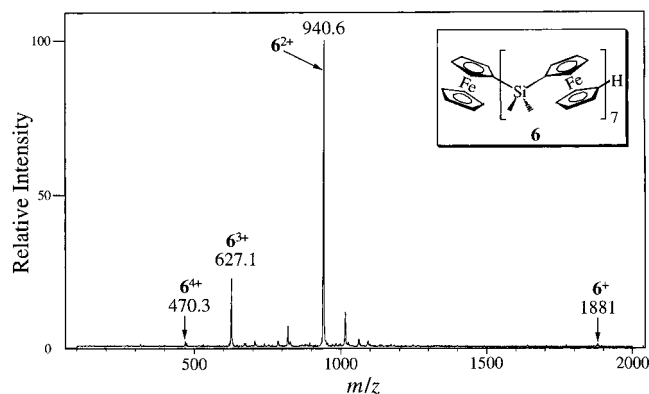


**Figure 9.** ESI mass spectrum of 10  $\mu\text{M}$  **6** with 0.25 mM lithium triflate (LiTrif) in 9:1 dichloromethane:acetonitrile (DCM:MeCN) at an infusion rate of 1.0  $\mu\text{L min}^{-1}$ . ESI voltage =  $-2583$  V and current = 50 nA.

+0.43 V vs SCE is observed for both the hexamer and octamer. The remaining ferrocene centers of both **5** and **6** can be oxidized ( $E_{1/2} \sim +0.54$  V vs SCE) without any evidence of precipitation in dichloromethane. Due to the virtually indistinguishable nature of the individual electron transfers of the first multielectron wave at  $E_{1/2} = +0.30$  V vs SCE for both **5** and **6**, ESI-MS results similar to those obtained for **4** are expected. That is to say the ESI spectra should display all of the redox charge states associated with the first voltammetric wave ( $M^+ - M^{3+}$  for **5** and  $M^+ - M^{4+}$  for **6**). As can be seen in Figure 8, the  $M^+$ ,  $M^{2+}$ , and  $M^{3+}$  of **5** are observed at a flow rate of 1  $\mu\text{L min}^{-1}$ . Analysis of the isotope spacing confirms the assignments. To our knowledge, this is the first example of a multiply charged ion containing more than two charges that was formed by electrolytic ESI. A comprehensive flow rate study was not undertaken, but  $5^{3+}$  was not observed with  $\nu \geq 1.5$   $\mu\text{L min}^{-1}$ . The ESI mass spectrum of **6** (Figure 9) exhibits ions that can be clearly assigned to the  $M^+$ ,  $M^{2+}$ ,  $M^{3+}$ , and  $M^{4+}$  species. As the analyte flow rate was increased, the intensities of the more highly charged ions were found to decrease, while those of the lower oxidation states increased. As expected, there was no evidence in any of the spectra that would indicate the presence of charge states greater than 4+.

In our previous discussion concerning calculation of  $E_{\text{wk}}$  during the ESI-MS experiments involving **2**, it was assumed that  $E_{\text{wk}}$  could be accurately determined through the use of *only*  $I_{2^+}/I_{2^+}$  and eq 8. It of course would be beneficial to have information regarding how much of the neutral species,  $2^0$ , is present, so that a cross-check of the value of  $E_{\text{wk}}$  could be

obtained. This is not possible for **2** using ESI-MS, but UV-vis spectroscopy might be able to aid in such an analysis.<sup>4c,25</sup> However, the ESI mass spectra of **5** and **6** should allow for independent determinations of  $E_{\text{wk}}$  using intensity ratios of the different charge states.<sup>26</sup> Upon comparing the values of  $E_{\text{wk}}$  determined from various charge state intensity ratios, it was found that the values were not self-consistent. In the case of **5** in Figure 8,  $E_{\text{wk}}$  is calculated to be  $-82$  mV when  $I_{5^{2+}}/I_{5^+}$  is used with eq 8 but is found to be  $-54$  and  $-24$  mV when  $I_{5^{3+}}/I_{5^+}$  and  $I_{5^{3+}}/I_{5^{2+}}$  are used, respectively. Similar discrepancies in  $E_{\text{wk}}$  for **6** (Figure 9) were noted;  $E_{\text{wk}}$  ranged from  $-30$  to  $-18$  mV. At this time, we do not have experimental evidence that would provide sufficient support for a reason as to why the ion intensities do not follow those predicted by eq 8. From our results with **3**, which demonstrated a high probability for charge reduction of  $3^{2+}$  upon entering the gas phase, it is quite possible that the more highly charged species of **5** and **6** undergo reactions that result in a lowering of the oxidation state. Even though the first voltammetric wave for both **5** and **6** exhibits but one discernible peak *in solution*, it is quite possible that species such as  $6^{4+}$  or  $5^{3+}$  will have an increasingly higher potential as more and more solvent is removed from around the cation during the desolvation process. This increase in oxidative capabilities would presumably lead to reactions of such highly charged analyte species with solvent or trace impurities. Regardless of the inconsistencies in the calculated values of  $E_{\text{wk}}$  for **5** and **6** and their origin, the fact that multiply charged species of compounds such as **5** and **6** can be obtained at reasonable flow rates and concentrations bodes well for the ESI-MS analysis of polymeric metallocenes and poly(heterocycles), such as poly(vinylferrocene) and poly(3-alkylthiophenes).

## Summary

The constant-current electrolytic nature of electrospray ionization mass spectrometry can be used to readily produce charged analytes with greater than two charges per molecule if the standard redox potential is the same for all of the redox centers in the molecule. Small changes in the analyte infusion rate are shown to have a large impact on the population of the various charge states, with higher flow rates resulting in decreased populations for the higher charge states. These changes in charge state population are apparently the result of changes in the potential of the electrospray needle, as noted in the case of a biferrrocene with two equivalent redox centers separated by 12 methylene units. The possible occurrence of charge-reducing reactions for a biferrrocene with two equivalent redox centers separated by two methylene units is suggested by the persistence of the singly charged species in the ESI mass spectra of analyte solutions that have excess added oxidant. The observation of up to four charges per molecule for an oligo(ferrocenylsilane) can be achieved, leading us to believe that ESI-MS will become an important tool in the analysis of redox-active polymers that exhibit solution voltammetry indicative of multiple electron transfer in a single event.

**Acknowledgment.** Professor Ian Manners and Ron Rulkens at the University of Toronto are gratefully acknowledged for generously donating the oligo(ferrocenyldimethylsilanes) for these studies. We thank the National Science Foundation (CHE-9529770) and the Louisiana Education Quality Support Fund for financial support of this work. Helpful discussions with Professor G. Cochran from the LSU Department of Mathematics are acknowledged.

## References and Notes

- (1) Smith, P. B.; Pasztor, Jr., A. J.; McKelvy, M. L.; Meunier, D. M.; Froelicher, S. W.; Wang, F. C.-Y. *Anal. Chem.* **1997**, *69*, 95R–121R.
- (2) (a) Dole, M.; Mack, L. L.; Hines, R. L.; Mobley, R. C.; Ferguson, L. D.; Alice, M. B. *J. Chem. Phys.* **1968**, *49*, 2240–2249. (b) Nohmi, T.; Fenn, J. B. *J. Am. Chem. Soc.* **1992**, *114*, 3241–3246. (c) Kallos, G. J.; Tomalia, D. A.; Hedstrand, D. M.; Lewis, S.; Zhou, J. *Rapid Commun. Mass Spectrom.* **1991**, *5*, 383–386. (d) O'Connor, P. B.; McLafferty, F. W. *J. Am. Chem. Soc.* **1995**, *117*, 12826–12831.
- (3) (a) Tanaka, K.; Waki, H.; Ido, Y.; Akita, S.; Yoshida, Y.; Yoshida, T. *Rapid Commun. Mass Spectrom.* **1988**, *2*, 151–153. (b) Bahr, U.; Deppe, A.; Karas, M.; Hillenkamp, F.; Giessmann, U. *Anal. Chem.* **1992**, *64*, 2866–2869. (c) Danis, P. O.; Karr, D. E.; Mayer, F.; Holle, A.; Watson, C. H. *Org. Mass Spectrom.* **1992**, *27*, 843–846. (d) Belu, A. M.; DeSimone, J. M.; Linton, R. W.; Lange, G. W.; Friedman, R. M. *J. Am. Soc. Mass Spectrom.* **1996**, *7*, 11–24.
- (4) (a) Van Berkel, G. J.; McLuckey, S. A.; Glish, G. L. *Anal. Chem.* **1991**, *63*, 1098–1109. (b) Van Berkel, G. J.; McLuckey, S. A.; Glish, G. L. *Anal. Chem.* **1992**, *64*, 1586–1593. (c) Van Berkel, G. J.; Zhou, F. *Anal. Chem.* **1995**, *67*, 2916–2923. (d) Van Berkel, G. J.; Zhou, F. *Anal. Chem.* **1995**, *67*, 3958–3964. (e) Van Berkel, G. J.; Zhou, F. *J. Am. Soc. Mass Spectrom.* **1996**, *7*, 157–162. (f) Van Berkel, G. J. In *Electrospray Ionization Mass Spectrometry: Fundamentals, Instrumentation, and Applications*; Cole, R. B., Ed.; Wiley-Interscience: New York, 1997; Chapter 2, pp 65–105.
- (5) Xu, X.; Nolan, S. P.; Cole, R. B. *Anal. Chem.* **1994**, *66*, 119–125.
- (6) Blades, A. T.; Ikononou, M. G.; Kebarle, P. *Anal. Chem.* **1991**, *63*, 2109–2114.
- (7) Bard, A. J.; Faulkner, L. R. In *Electrochemical Methods: Fundamentals and Applications*; Wiley: New York, 1980.
- (8) Curran, D. J. In *Laboratory Techniques in Electroanalytical Chemistry*; 2nd ed.; Heineman, W. R., Kissinger, P., Eds.; Marcel Dekker: New York, 1996.
- (9) (a) DuPont, A.; Gisselbrecht, J.-P.; Leize, E.; Wagner, L.; Van Dorsselaer, A. *Tetrahedron Lett.* **1994**, *35*, 6083–6086. (b) McCarley, T. D.; DuBois, C. J.; McCarley, R. L. *Proceedings of the 44th ASMS Conference on Mass Spectrometry and Allied Topics*, Portland, OR, May 12–16, 1996; p 1011. (c) Vandell, V. E.; Limbach, P. A. *J. Mass Spectrom.* **1998**, *33*, 212–220.
- (10) (a) *Handbook of Conducting Polymers*, 2nd ed.; Skotheim, T. A., Elsenbaumer, R. L., Reynolds, J. R., Eds.; Marcel Dekker: New York, 1996. (b) *Handbook of Conducting Polymers*; Skotheim, T. A., Ed.; Marcel Dekker: New York, 1986. (c) Murray, R. W.; Ewing, A. G.; Durst, R. A. *Anal. Chem.* **1987**, *59*, 379A–385A.
- (11) (a) Murray, R. W. *Annu. Rev. Mater. Sci.* **1984**, *14*, 145–169. (b) Abruña, H. D.; Denisevich, P.; Umaña, M.; Meyer, T. J.; Murray, R. W. *J. Am. Chem. Soc.* **1981**, *103*, 1–5.
- (12) (a) Diaz, A. F.; Kanazawa, K. K. *J. Chem. Soc., Chem. Commun.* **1979**, 635–636. (b) Diaz, A. F.; Logan, J. A. *J. Electroanal. Chem.* **1980**, *111*, 111–114. (c) Diaz, A. F. *Chem. Scr.* **1981**, *17*, 145–148.
- (13) Kanatzidis, M. G. *Chem. Eng. News* **1990**, Dec 3, 36–54.
- (14) (a) Sato, M.; Tanaka, S.; Kaeriyama, K. *J. Chem. Soc., Chem. Commun.* **1985**, 713–714. (b) Miller, G. G.; Elsenbaumer, R. L. *J. Chem. Soc., Chem. Commun.* **1986**, 1346–1347. (c) Roncali, J.; Garnier, F. J. *J. Chem. Soc., Chem. Commun.* **1986**, 783–784. (d) Sato, M.; Tanaka, S.; Kaeriyama, K. *J. Chem. Soc., Chem. Commun.* **1986**, 873–874. (e) Bryce, M. R.; Chissel, A.; Kathirgamanathan, P.; Parker, D.; Smith, N. R. M. *J. Chem. Soc., Chem. Commun.* **1987**, 466–467. (f) Hotta, S.; Rughooputh, S. D. D. V.; Heeger, A. J.; Wudl, F. *Macromolecules* **1987**, *20*, 212–215. (g) McCulloch, R. D.; Lowe, R. D. *J. Chem. Soc., Chem. Commun.* **1992**, 70–72. (h) McCulloch, R. D.; Tristram-Nagle, S.; Williams, S. P.; Lowe, R. D.; Jayaraman, M. *J. Am. Chem. Soc.* **1993**, *115*, 4910–4911. (i) Taj, S.; Ahmed, M. F.; Sankarapavinasam, S. *J. Electroanal. Chem.* **1992**, *338*, 347–352. (j) Miyaura, N.; Yanagi, T.; Suzuki, A. *Synth. Commun.* **1981**, *11*, 513–519. (k) Leclerc, M.; Diaz, F. M.; Wegner, G. *Makromol. Chem.* **1989**, *190*, 3105–3116. (l) Heffner, G. W.; Pearson, D. S. *Macromolecules* **1991**, *24*, 6295–6299.
- (15) (a) Lufaso, M. W.; Curtin, L. S. Manuscript in preparation. (b) Morrison, Jr., W. H.; Krogsrud, S.; Hendrickson, D. N. *Inorg. Chem.* **1973**, *12*, 1998–2004.
- (16) (a) Rulkens, R.; Lough, A. J.; Manners, I.; Lovelace, S. R.; Grant, C.; Geiger, W. E. *J. Am. Chem. Soc.* **1996**, *118*, 12683–12695. (b) Foucher, D. A.; Tang, B. Z.; Manners, I. *J. Am. Chem. Soc.* **1992**, *114*, 6246–6248.
- (17) (a) Flanagan, J. B.; Margel, S.; Bard, A. J.; Anson, F. C. *J. Am. Chem. Soc.* **1978**, *100*, 4248–4253. (b) Itaya, K.; Bard, A. J.; Szwarc, M. *Z. Phys. Chem. (Munich)* **1978**, *112*, 1–9.
- (18) Whitehouse, C. M.; Dreyer, R. N.; Yamashita, M.; Fenn, J. B. *Anal. Chem.* **1985**, *57*, 675–679.
- (19) (a) Chidsey, C. E. D.; Bertozzi, C. R.; Putvinski, T. M.; Majsce, A. M. *J. Am. Chem. Soc.* **1990**, *112*, 4301–4306. (b) Creager, S. E.; Hockett, L. A.; Rowe, G. K. *Langmuir* **1992**, *8*, 854–861.
- (20) Although it is possible that slow electron transfer at the solution/electrode interface could affect production of  $M^{2+}$ , we do not consider these effects to be significant.
- (21) Van Berkel, G. J.; Zhou, F. *Proceedings of the 45th ASMS Conference on Mass Spectrometry and Allied Topics*, Palm Springs, CA, June 1–5, 1997; p 371.
- (22) With the analyte infusion rates used here, we calculate that the flow in the electrospray needle should be laminar. In addition, we have assumed that the analyte flowing through the electrospray needle experiences a current that is less than the mass-transport limited current,  $i_{lim}$ . Under these conditions, the potential of the working electrode can be estimated to be  $E_{wk} = E^0 + (RT/nF) \ln[i/(i_{lim} - i)]$  with the current being defined by  $i = -nFC^0_k v [1 - e^{-A/v}]$  where  $A$  is a constant that depends on the mass-transport characteristics of the analyte and dimensions of the electrospray needle.
- (23) We realize that without knowledge of the population of  $M^0$  present that our values may be in error. This is discussed in more detail in the section on the oligo(ferrocenyldimethylsilanes).
- (24) McCarley, T. D.; McCarley, R. L. *Anal. Chem.* **1997**, *69*, 130–136.
- (25) Connelly, N. G.; Geiger, W. E. *Chem. Rev.* **1996**, *96*, 877–910.
- (26) From a statistical point of view, the hexamer and the octamer can be treated as a trimer and a tetramer, respectively, for the first electron-transfer event. That is to say that the population of a given charge state for the first electron-transfer event will not be affected by the presence of the other ferrocene sites that will be oxidized at a higher potential. Thus, the charge state populations were calculated for **5** and **6** using eq 8 with  $n = 3$  and 4, respectively.